

## Metabolomics reveal the mechanism for anti-renal fibrosis effects of an *n*-butanol extract from *Amygdalus mongolica*

CHEN GAO<sup>1,2,a</sup>  
HONG CHANG<sup>1,a</sup>  
HONG-BING ZHOU<sup>1</sup>  
QING LIU<sup>1</sup>  
YING-CHUN BAI<sup>1</sup>  
QUAN-LI LIU<sup>1,3</sup>  
WAN-FU BAI<sup>1,\*</sup>  
SONG-LI SHI<sup>1,3\*</sup>

<sup>1</sup> Department of Pharmacy, Baotou Medical College, Baotou, Inner Mongolia China, 014040

<sup>2</sup> Department of Pharmacy, The Second Affiliated Hospital of Baotou Medical College, China, 014030

<sup>3</sup> Institute of Bioactive Substance and Function of Mongolian Medicine and Chinese Materia Medica, Baotou Medical College, Baotou, Inner Mongolia, China 014040

To reveal the mechanism of anti-renal fibrosis effects of an *n*-butanol extract from *Amygdalus mongolica*, renal fibrosis was induced with unilateral ureteral obstruction (UUO) and then treated with an *n*-butanol extract (BUT) from *Amygdalus mongolica* (Rosaceae). Sixty male Sprague-Dawley rats were randomly divided into the sham-operated, renal fibrosis (RF) model, benazepril hydrochloride-treated model (1.5 mg kg<sup>-1</sup>) and BUT-treated (1.75, 1.5 and 1.25 g kg<sup>-1</sup>) groups and the respective drugs were administered intragastrically for 21 days. Related biochemical indices in rat serum were determined and histopathological morphology observed. Serum metabolomics was assessed with HPLC-Q-TOF-MS. The BUT reduced levels of blood urea nitrogen, serum creatinine and albumin and lowered the content of malondialdehyde and hydroxyproline in tissues. The activity of superoxide dismutase in tissues was increased and an improvement in the severity of RF was observed. Sixteen possible biomarkers were identified by metabolomic analysis and six key metabolic pathways, including the TCA cycle and tyrosine metabolism, were analyzed. After treatment with the extract, 8, 12 and 9 possible biomarkers could be detected in the high-, medium- and low-dose groups, respectively. Key biomarkers of RF, identified using metabolomics, were most affected by the medium dose. *A. mongolica* BUT extract displays a protective effect on RF in rats and should be investigated as a candidate drug for the treatment of the disease.

**Keywords:** *Amygdalus mongolica*, renal fibrosis, protective effect, metabolomics, mechanism

Accepted September 14, 2021  
Published online September 15, 2021

Renal fibrosis (RF) is a major health threat globally. Ten percent of the human population is affected by chronic kidney disease (CKD) and RF (1, 2). RF is the final common pathway of various renal injuries, leading to CKD and end-stage renal disease (3). Therefore, inhibiting renal fibrosis could delay or prevent CKD (4). Currently, very few therapeutics

\* Correspondence; e-mail: 102010114@btmc.edu.cn; shisongli122@126.com

<sup>a</sup> These authors contributed equally to this work.

are available for effective RF treatment. Traditional Chinese medicine (TCM) formulations are promising alternatives for the prevention and treatment of RF (5). Exploring RF treatment with TCM is gaining attention in the medical community. More importantly, the mechanistic basis of TCM action has been increasingly elucidated through metabolomics. Finding biomarkers for early diagnosis and drugs for RF intervention has become a research emphasis (6).

*Amygdalus mongolica* Maxim, family Rosaceae, is a deciduous shrub native to the Mongolian Plateau (7, 8). The seeds of *A. mongolica*, used as “Yu Li Ren” (*Pruni semen*, a traditional Chinese medicine), have been used for the treatment of cough and for reducing phlegm production, constipation and edema (9). Yu Li Ren is a TCM used in the adjuvant treatment of nephropathy and glomerulonephritis (10, 11). Recent reports have shown that *A. mongolica* contains amygdalin, alkaloids and other pharmacological components (5). Previous studies showed that the content of amygdalin in the *n*-butanol extract (BUT) of *A. mongolica* was 47.72 %. BUT can counter lipid peroxidation, reduction of oxidative stress and certain protective effects on the liver and its effective dose range is 1.02.0 g kg<sup>-1</sup> (12, 13). Studies have documented that amygdalin can induce cell apoptosis and is a potent anti-fibrotic agent. Amygdalin has been used to treat different types of cancers and organ fibrosis (12). A recent study showed that *A. mongolica* total extract (TOT) had the effect of anti-renal fibrosis in rats (13). In addition, the petroleum ether and BUT of *A. mongolica* were the effective active sites to prevent pulmonary fibrosis and RF (5, 14–16). However, the mechanisms underlying the antifibrotic effects of *A. mongolica* BUT are still unclear. Thus, metabolomics technology was used to study the mechanism and dose of the *A. mongolica* BUT on RF in this research, in order to find the optimal dose.

Metabolomics analyzes a broad spectrum of metabolites to illustrate changes in metabolite profiles to clarify relationships between metabolites and corresponding physiological and pathological states. The approach can be used to screen for sensitive biomarkers and is a powerful tool for examining the efficacy of TCM and for identifying mechanisms of drug action (17). TCM metabolism is a dynamic process due to multiple components and targets, which make it complex with extensive efficacy output. Bridging metabolism and TCM efficacy is necessary to address important problems in TCM research; metabolomics has obvious advantages for studying the basis and mechanism of action of TCM (18, 19).

## EXPERIMENTAL

### *Chemicals and reagents*

The seeds of *A. mongolica* were collected from Alashan Yabulai Gobi (104°48'09" E 40°11'24"N) and identified as *A. mongolica* by Professor Shi Song-li of School of Pharmacy, Baotou Medical College. Following reagents were purchased: benazepril hydrochloride (Beijing Novartis Pharmaceutical Co., Ltd., China); pentobarbital sodium (Merck, Germany); sodium carboxymethyl cellulose (Analytical Pure, Tianjin Kaitong Chemical Reagent Co., Ltd., China); penicillin sodium for injection (North China Pharmaceutical Co., Ltd., China, batch number: F7116323); HE and Masson dyeing kits (Nanjing Jiancheng Technology Co., Ltd., China); methanol (LC-MS grade, Honeywell, USA, 67-56-1); acetonitrile (LC-MS grade, Honeywell, 75-05-8); and formic acid (LC-MS grade, Sigma-Aldrich, USA, 64-18-6).

### *Animals, groups and treatment*

Sixth SPF grade SD male rats weighing 170–200 g were purchased from the Department of Medical Sciences of Peking University, license number SCXK (Beijing, China) 2011 Mel 0012.

Animal studies were approved by the Ethics Committee of Baotou Medical College (approval number: 20190314). After 1 week of adaptive feeding, 60 SD rats were randomly divided into 6 groups: disease model group (MOD), sham operation group (SDG), benazepril-treated group (BH, 1.5 mg kg<sup>-1</sup>) and the high (BUT-H, 1.75 g kg<sup>-1</sup>), medium (BUT-M, 1.5 g kg<sup>-1</sup>) and low (BUT-L, 1.25 g kg<sup>-1</sup>) dose groups (*n* = 10 for each group). The rat disease model of renal fibrosis was prepared by unilateral ureteral obstruction (UUO) (20). The MOD is used to estimate differences with SDG and used for pharmacology studies. Only the left ureter was separated but not ligated and the abdominal cavity was closed in the sham operation group (SDG) for normal control. The animals in the SDG and MOD groups were daily given an oral gavage of 4 mL normal saline instead of plant extract. The benazepril, as a positive control drug, has a good renoprotective effect in RF (21), which was used to compare the efficacy of *n*-butanol extract. Treatments, including BH, BUT-H, BUT-M, BUT-L, were administered by intragastric gavage, once a day at the same time for 21 days.

The LD<sub>50</sub> of amygdalin was approximately 522 mg kg<sup>-1</sup> (12). The contents of amygdalin were 233, 200 and 167 mg kg<sup>-1</sup>, in the high, medium and low dose BUT groups, respectively.

### *Preparation of n-butanol extract of A. mongolica and chemical analysis*

The *n*-butanol extract of *A. mongolica* was prepared according to the published method (16). The BUT extract liquor was concentrated using rotary evaporation (27.95 % yield). BUT was dissolved in 0.5 % sodium carboxymethyl cellulose to prepare high, medium and low dose groups with concentrations of 0.098, 0.084 and 0.07 g mL<sup>-1</sup>, respectively.

The *A. mongolica* BUT was separated and purified using the chromatographic and spectroscopic methods as described in previous studies. Finally, amygdalin was isolated and shown to account for 47.72 % of the BUT content in *A. mongolica* (16).

### *Animal specimen collection*

The animals were weighed and anaesthetized using an intraperitoneal injection of 3 % pentobarbital 24 h after the last drug administration. Blood was drawn from the abdominal aorta and centrifuged at 3000 rpm for 10 min. The serum for biochemical and metabolomic analysis, the left kidney for lobe histopathology analysis was collected according to previous studies (13, 16).

### *Determination of biochemical indexes and pathological analysis*

Biochemical indexes detection and histological examination were as described in previous studies (13, 22).

### *UPLC-Q-TOF/MS assay*

Liquid phase gradient elution conditions and the mass spectrometry conditions were as in previous studies (16).

### Data analysis

The raw data processing and candidate identification were the same as for previous studies (16). Principal component analysis (PCA) and partial least squares discriminant analysis (PLS-DA) were used to visually analyze cluster results and potential biomarkers were screened using values of variable importance of projection (VIP) and *t*-tests. The metabolic pathways of differentially altered metabolites were analyzed by MetPA using MetaboAnalyst software 4.0. Metabolites in these pathways were selected as key biomarkers for RF. Levels of biomarkers were analyzed by ROC with GraphPad Prism 5 to test diagnostic power.

The software SPSS 17.0 was used to analyze the experimental data and the experimental results are expressed as means  $\pm$  SD.

## RESULTS AND DISCUSSION

Recent studies showed that BUT of *A. mongolica* was effective in the prevention of RF (5, 13–16). However, the optimal dose and the mechanisms underlying the antifibrotic effects of BUT are still unclear. In this study, the effects of high, medium and low doses of BUT on the biochemical parameters and histopathology of renal fibrosis rats were investigated in a preliminary experiment. The metabolomics studies were conducted to further explore their mechanism, in order to find the optimal dose.

### Effects of *n*-butanol extract on biochemical indexes levels

Biochemical assays were performed to assess the effect of drug treatment on the kidney functions of rats. For positive control, we chose benazepril, an angiotensin II inhibitor that reduces plasma aldosterone levels, increases vasodilatation, lowers blood pressure, relieves oxidative stress, increases glomerular filtration rate and reduces proteinuria (5). As shown in Fig. 1, the levels of serum blood urea nitrogen (BUN), serum creatinine (Scr), serum albumin (ALB) and tissue superoxide dismutase (SOD) and hydroxyproline (HYP) were significantly higher in the MOD *versus* SDG groups, whereas the tissue SOD activity was significantly reduced ( $p < 0.01$ ), indicating successful RF modelling. In the current study, we demonstrated that treatment with BH, as well as the low and medium doses of BUT, showed protective effects against UUO-induced kidney injury *in vivo*. These results displayed serum BUN, Scr, ALB, tissue MOD and HYP levels were significantly decreased, but SOD activities were significantly increased ( $p < 0.01$ ). Thus, BUT reduces damage to renal tubular cells, inhibits free radical accumulation, alleviates lipid peroxidation, delays fibrosis and protects rats from RF induced by UUO. BUT-L and BUT-M showed the most significant effect ( $p < 0.01$ ).

### Pathological changes of kidney tissue

Histopathologic changes in renal tissue were obviously caused by the degree of renal injury and fibrosis (5). Renal injury was analyzed using the HE and Masson stain, as seen in Fig. 2. There were no abnormal pathological changes in glomerular structure or renal tubules of the SDG rats, while the UUO rats exhibited severe tubular atrophy, interstitial

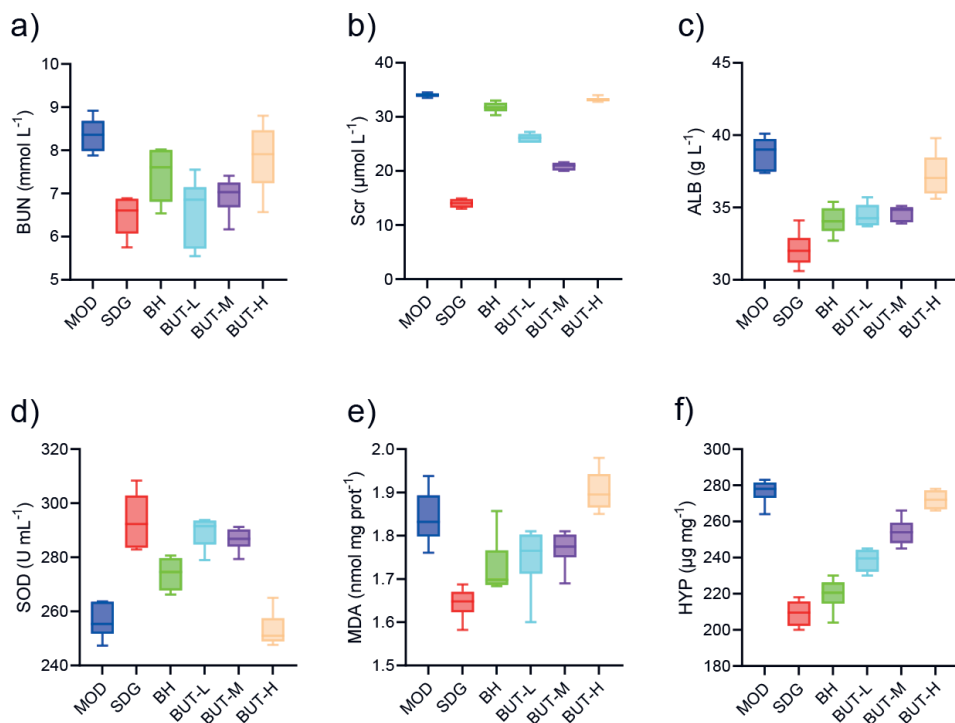


Fig. 1. Serum or tissue levels of biochemical markers in rats treated with different *A. mongolica* extracts: a) levels of blood urea nitrogen (BUN), b) levels of serum creatinine (Scr), c) levels of serum albumin (ALB), d) activity of superoxide dismutase (SOD), e) content of malondialdehyde (MDA), f) content of tissue hydroxyproline (HYP). All values represent the mean  $\pm$  SD. \* $p < 0.05$ , \*\* $p < 0.01$  compared to the MOD group. #  $p < 0.05$  and ##  $p < 0.01$  compared to the SDG group. MOD: disease model group; SDG: sham operation group; BH: benazepril-treated group; BUT-H: *n*-butanol extract high dose group; BUT-M: *n*-butanol extract middle dose group; BUT-L: *n*-butanol extract low dose group.

fibrosis and inflammation (16). Treatment with BH, BUT-L, BUT-M and BUT-H reduced renal interstitial inflammatory and interstitial fibrosis alleviated. Consistent with the results of biochemical indices, BUT-L and BUT-M showed the most significant effect ( $p < 0.01$ ). The content of amygdalin was  $233 \text{ mg kg}^{-1}$ , in the high dose group of BUT, which was close to the LD50 of amygdalin  $552 \text{ mg kg}^{-1}$ . Taken together, both BH and the low and medium doses of BUT can protect kidney tissues from UUO-induced fibrosis.

#### Cluster analysis of serum metabolic spectra in experimental groups

In this study, serum blood samples from each group were analyzed *via* a metabolomics approach, using UPLC-Q-TOF/MS followed by multivariate data analysis by means of PCA and PLS-DA (Fig. 3). The PCA diagram directly illustrates distinctions among samples (Fig. 3a,b). As shown in the PCA score plots, all groups in this study were clustered; MOD and SDG are obviously separated; BUT-L, BUT-M and BUT-H were distinct

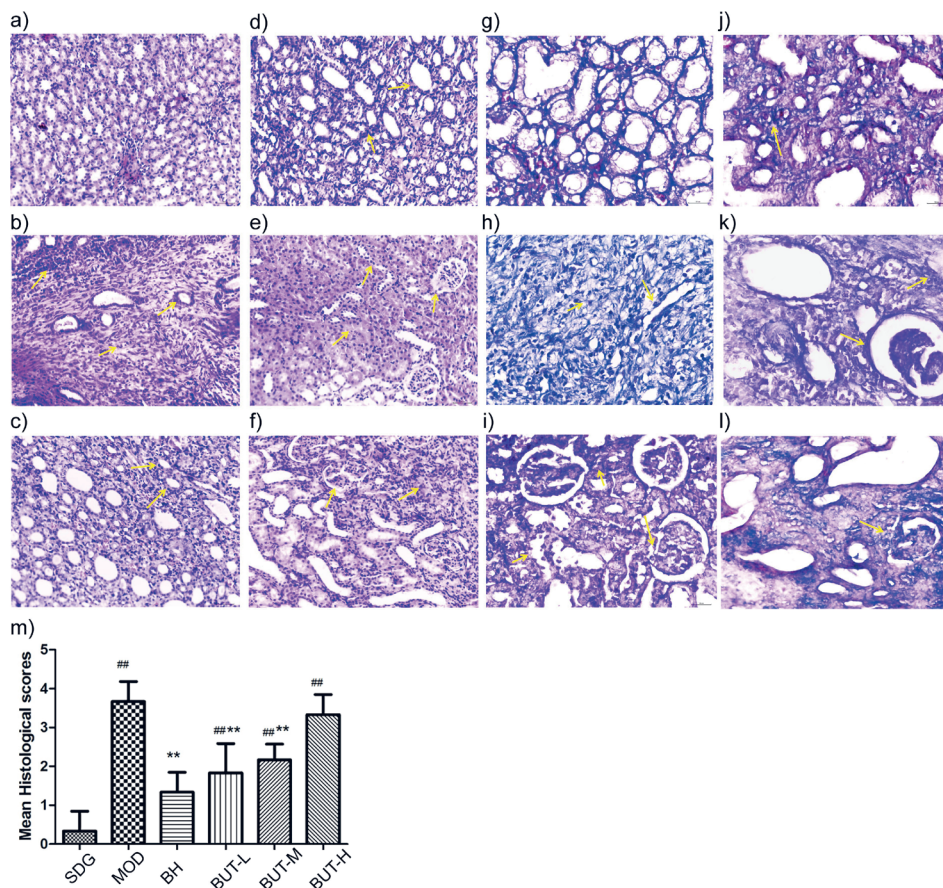


Fig. 2. Pathological changes in renal tissue: a)–f), m) representative images of HE staining ( $\times 200$ ) and score; g)–l) representative images of Masson dyeing ( $\times 200$ ), a), g) SDG, b), h) MOD, c) i) BH, d), j) BUT-L, e), k) BUT-M, f), l) BUT-H. Values represent the mean  $\pm$  SD. \* $p < 0.05$  and \*\* $p < 0.01$  compared to the MOD group. #  $p < 0.05$  and ##  $p < 0.01$  compared to the SDG group. MOD: disease model group; SDG: sham operation group; BH: benazepril-treated group; BUT-H: *n*-butanol extract high dose group; BUT-M: *n*-butanol extract middle dose group; BUT-L: *n*-butanol extract low dose group.

from MOD and closer to SDG. Next, we performed supervised PLS-DA to maximize the separation between each group (Fig. 3c,d). PLS-DA, on the other hand, showed further separation of MOD from SDG, BUT-L, BUT-M and BUT-H. The treatment groups were closer to SDG and BUT-M being the most similar, consistent with pharmacological results.

#### Screening and identification of potential biomarkers

As shown in the PCA (Fig. 4a,b) and PLS-DA (Fig. 4c,d) score plots, MOD and SDG had good differentiation in both the positive and negative ion modes, which indicated distinct

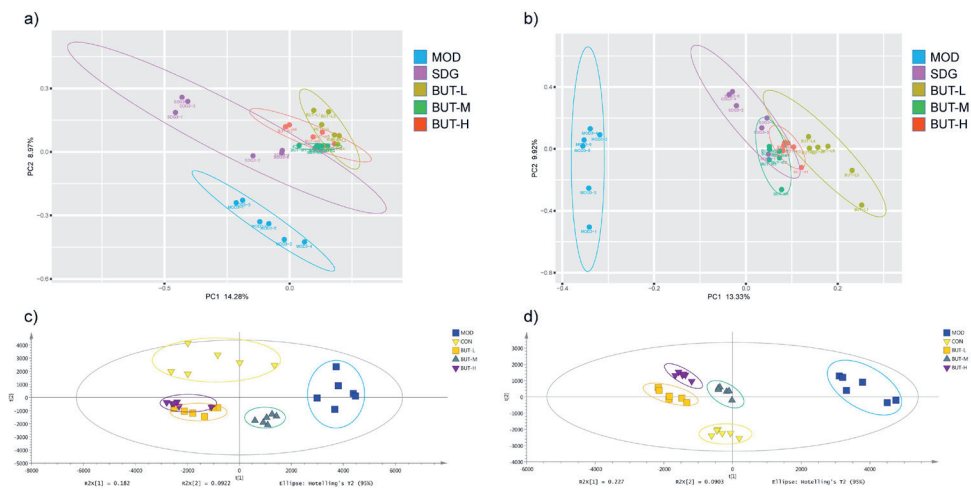


Fig. 3. PCA and PLS-DA score plots of SDG, MOD, BH, BUT-L, BUT-M and BUT-H: a), b) PCA score plot in positive and negative ion mode respectively, c), d) PLS-DA score plot in positive and negative ion mode respectively. The circles represent their respective cluster of samples within the same group. MOD: disease model group; SDG: sham operation group; BH: benazepril-treated group; BUT-H: *n*-butanol extract high dose group; BUT-M: *n*-butanol extract middle dose group; BUT-L: *n*-butanol extract low dose group.

metabolomic profiles (5). The V-plot map (Volcano Plot) (Fig. 4e-l) of MOD compared with SDG, BUT-L, BUT-M and BUT-H obtaining 1285, 1589, 1314 and 1351 differential metabolites, respectively. Based on pharmacological and metabolomic results described above, BUT-M showed advantages in anti-renal fibrosis. Therefore, this paper compared MOD and BUT-M to investigate the mechanism of BUT anti-renal fibrosis. Finally, sixteen differentially abundant metabolites (10 in positive ion mode and 6 in negative ion mode) were detected in the model group relative to the BUT-M based on  $VIP > 1$  and  $p < 0.05$  (Supplementary Table I, 5a) and their content variations were shown in a heat map (Fig. 5b). A Venn diagram (Fig. 5c) shows the results of potential biomarkers for significant callbacks in each group. BUT-H, BUT-M and BUT-L could respectively callback 9, 12 and 8 potential biomarkers while simultaneously acting on 6 of the same potential biomarkers together. From this, the medium-dose ( $1.5 \text{ g kg}^{-1}$ ) was more effective in normalizing or reversing metabolites.

### Diagnostic potential of key metabolites

ROC analysis further verified the diagnostic potential of sixteen potential biomarkers in MOD compared to BUT-M:  $0.7 < AUC < 0.9$  indicates the diagnostic accuracy of a biomarker;  $AUC > 0.9$  indicates a very high accuracy. Except for alpha-CEHC ( $AUC = 0.5556$ ), the  $AUC$  values of the other fifteen potential diagnostic biomarkers were greater than 0.7 and all fifteen metabolites displayed diagnostic accuracy (Fig. 5d,e).

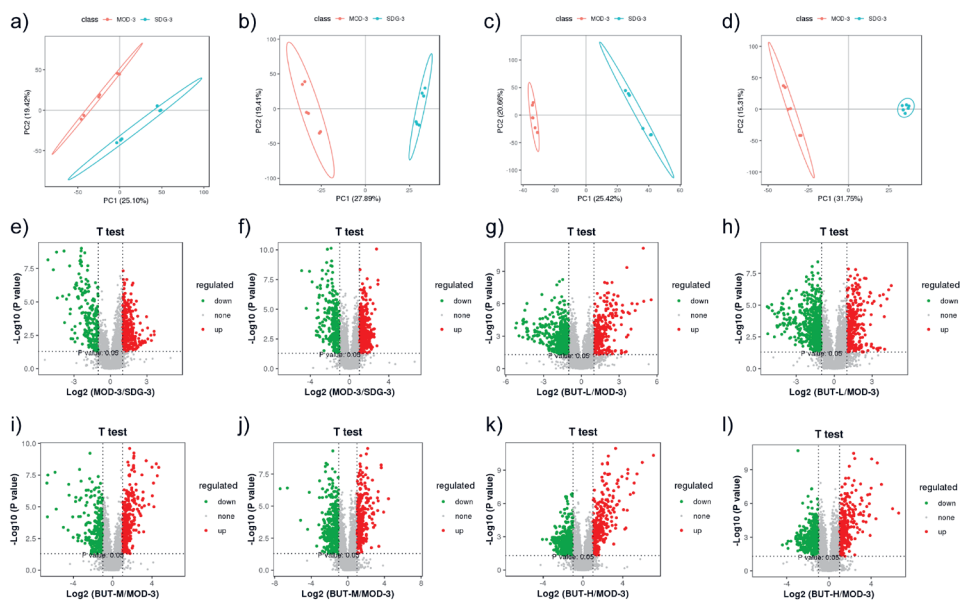


Fig. 4. a), b) PCA diagram showing good clustering of samples within the same group in positive and negative ion mode of MOD and SDG (5), c), d) PLS-DA diagram in positive and negative ion mode of MOD compared with SDG, e)–l) volcano plot map in positive and negative ion mode of MOD compared with SDG, BUT-L, BUT-M and BUT-H. MOD: disease model group, SDG: sham operation group, BH: benazepril-treated group, BUT-H: *n*-butanol extract high dose group, BUT-M: *n*-butanol extract middle dose group, BUT-L: *n*-butanol extract low dose group.

### Analysis of related metabolic pathways and screening of key biomarkers

Metabolomic pathway analysis was further performed for the fifteen potential diagnostic metabolites using the MetPA web-based tool to identify crucial biomarkers. As shown in Fig. 5f, six metabolic pathways were markedly dysregulated ( $-\log P) > 2$  and  $\text{impact} > 0.02$ ). Finally, five crucial serum metabolites were identified from these pathways (Supplementary Table II). Metabolomics analyses showed that BUT-M mainly targets six metabolic pathways, which are affected during RF and lead to aberrant levels of succinic acid, L-tyrosine, bilirubin, L-cystathionine and mevalonic acid. The medium BUT dose was effective on all six metabolic pathways and restored the key biomarkers, therefore, we considered it the optimal dose for antifibrotic effects.

Metabolomic results showed that BUT-M decreased the level of succinic acid and acts on the citrate (TCA) cycle. In this pathway, succinic acid enters the TCA cycle, affecting tyrosine metabolism, cysteine and methionine metabolism and porphyrin and chlorophyll metabolism pathways. Further, BUT-M decreased the level of L-tyrosine and bilirubin and increased the level of L-cystathionine. Succinic acid is used as an antispasmodic, expectorant and diuretic. L-cystathionine is produced by the reaction of *O*-succinyl homoserine with cysteine. Mingzhu Zhu (23) and others have shown that L-cystathionine inhibits the



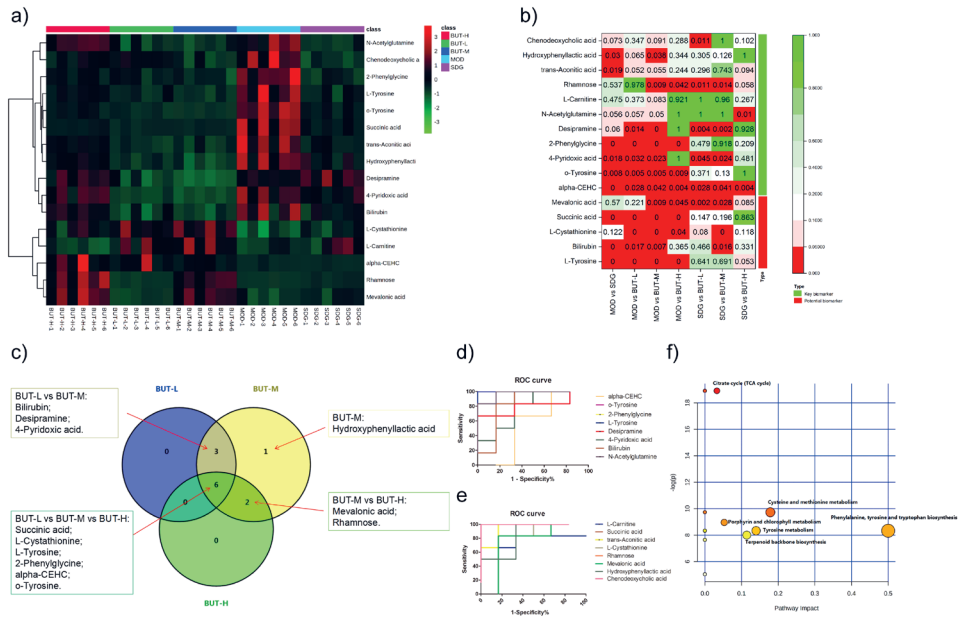


Fig. 5. Differential analysis of metabolite and metabolic pathway analysis of crucial biomarkers: a) Heat map of the differentially abundant metabolites in all groups. The degree of colour saturation indicates the metabolite expression with green and red, respectively indicating the lowest and highest expression, b) *p*-value heat map of the differential abundance of metabolites in all groups. The degree of colour saturation indicates intergroup differences in metabolite expression values with green and red respectively indicating non-significant and significant differences, c) Venn diagram of BUT-L, BUT-M and BUT-H biomarkers. Standard red is a key biomarker, d, e) ROC analysis of 13 potential biomarkers, f) metabolic pathway analysis of crucial biomarkers. BUT-H: *n*-butanol extract high dose group; BUT-M: *n*-butanol extract middle dose group; BUT-L: *n*-butanol extract low dose group.

expression of MCP-1/THP-1-derived ox-LDL and exerts its anti-inflammatory effect. Bilirubin is the main metabolite of iron porphyrin compounds *in vivo* that can inhibit the oxidation of linoleic acid and phospholipids. Hou-Dong (24) and other researchers have shown that bilirubin alleviates bleomycin-induced pulmonary fibrosis by inhibiting pulmonary inflammation. L-Tyrosine is a non-essential amino acid and a precursor of various bioactive substances (25). In this study, the levels of succinic acid, L-tyrosine and bilirubin were significantly increased while L-cystathionine was significantly decreased in the MOD group compared with those in the SDG group. The levels were efficiently restored to the control levels following treatment with BUT-M. This result demonstrates that BUT-M exhibited a significant protective effect on RF.

L-Tyrosine enters tyrosine metabolism and then affects the terpenoid backbone biosynthesis. In this pathway, an increased level of mevalonic acid affects the occurrence and development of RF. Farhan Rizvi (26) have shown that simvastatin inhibits the proliferation of human atrial fibroblasts. In this study, the levels of mevalonic acid were signifi-

cantly decreased in the MOD group compared with those in the SDG group. They were efficiently restored to the control levels after treatment with BUT-M. This result indirectly reflects an increased level of mevalonic acid in UUO rats and demonstrates that BUT-M exhibited a significant protective effect on RF.

## CONCLUSIONS

In this study, metabolomics technologies based on UPLC-QTOF-MS along with biochemical and histopathological analyses were used to reveal the effect and mechanism of *A. mongolica* BUT against RF in UUO rats. The results showed that BUT has anti-renal fibrosis effects, the medium dose (1.5 g kg<sup>-1</sup>) was the optimal dose. *A. mongolica* BUT inhibited RF and improved renal function by restoring five key biomarkers and six metabolic pathways, which are likely involved in inhibiting the release of inflammatory factors, reducing the oxidative stress response and inhibiting the proliferation of fibroblasts. This study provides the experimental basis for the clinical application of *A. mongolica* BUT.

*Acknowledgment.* – This work was supported by the National Natural Science Foundation of China [81641137 and 81760782], “Grassland Talents” Youth Innovation and Entrepreneurship Talent Project of Inner Mongolia Autonomous Region [Q2017046], The 11th “Grassland Talents” Talent Project of Inner Mongolia Autonomous Region [(2021)8], Natural Science Foundation of Inner Mongolia [2019MS08189, 2018LH03027, 2020MS08078, 2021LHMS08013 and 2021MS08050], Scientific Research Fund Project of Baotou Medical College [No. BYJJ-YF 201706], Doctoral Research Foundation of Baotou Medical College [No. BSJJ201814], Scientific Research Project of Inner Mongolia Autonomous Region [NJZY21048] and Inner Mongolia College Student Innovation and Entrepreneurship Training Program (S202119127004).

## REFERENCES

1. B. D. Humphreys, Mechanisms of renal fibrosis, *Annu. Rev. Physiol.* **80** (2018) 309–326; <https://doi.org/10.1146/annurev-physiol-022516-034227>
2. D. F. Xia, H. L. Qun, H. Di and Z. X. Zhi. Establishment and assessment on recanalization of unilateral ureteral occlusion model in sprague dawley rat, *Chin. J. Comparative Med.* **3** (2010) 30–35; <https://doi.org/10.3969/j.issn.1671-7856.2010.03.008>
3. A. N. Sun, W. Y. Kim, W. K. Jin, H. P. Sang, L. K. Hong, M. S. Lee, M. Komatsu, H. Ha, H. L. Ji and C. W. Park, Autophagy attenuates tubulointerstitial fibrosis through regulating transforming growth factor- $\beta$  and NLRP3 inflammasome signaling pathway, *Cell Death Dis.* **10** (2019) 78; <https://doi.org/10.1038/s41419-019-1356-0>
4. M. K. Elena, A. T. Omar Emiliano, T. Edilia and P. C. José, Unilateral ureteral obstruction as a model to investigate fibrosis-attenuating treatments, *Biomolecules* **9** (2019) 141; <https://doi.org/10.3390/biom9040141>
5. C. Gao, W. F. Bai, H. B. Zhou, H. M. Hao, Y. C. Bai, Q. L. Liu, H. Chang and S. L. Shi, Metabolomic assessment of mechanisms underlying anti-renal fibrosis properties of petroleum ether extract from *Amygdalus mongolica*, *Pharm. Biol.* **59** (2021) 565–574; <http://doi.org/10.1080/13880209.2021.1920619>
6. L. Qi, T. Yi, X. N. Wang, P. Liu and C. H. Liu, A Study on regularity of compound herbal formulae for renal fibrosis based on literature, *Chin. J. Info. Trad. Chin. Med.* **21** (2014) 34–37; <https://doi.org/10.3969/j.issn.1005-5304.2014.12.010>

7. Hohhot and P. R. C. Study on floristic geographical distribution of *Amygdalus mongolica*, *Actaentiarum Naturalium Univer Nmongol* **26** (1995) 713–715; <https://doi.org/10.19540/j.cnki.cjcm.20181225.001>
8. Khasbagan, J. Y. He, T. J. Wang, X. U. Jie, Soyolt, J. N. Wang and H. Zhao, Research progress of angiosperm flora of inner mongolia in the post-flora time, *J. Minzu. Univer. China* **19** (2010) 7–15; <https://doi.org/10.3969/j.issn.1005-8036.2010.03.001>
9. Z. Z. Yan, A. D. Li, D. L. Li and C. L. Li, Growth characteristics of endangered *Amygdalus mongolica*, *Acta Botanica Boreali-Occidentalia Sin.* **27** (2007) 0625–0628; <https://doi.org/10.3321/j.issn:1000-4025.2007.03.036>
10. J. Xie, Z. Zhang, T. X. Li, D. X. Kong and G. Z. Wang, Comparison analysis of amygdalin in the water decoction of *Pruni* semen and processed *Pruni* semen, *Chin. J. Hosp. Pharm.* **38** (2018) 2031–2033; <https://doi.org/10.13286/j.cnki.chinhosp pharmacy.2018.19.10>
11. I. H. Page, The effect on renal efficiency of lowering arterial blood pressure on cases of essential hypertension and nephritis, *J. Clin. Invest.* **13** (1934) 909–915; <https://doi.org/10.1172/JCI100635>
12. J. Wang, H. B. Zhou, T. Wu, P. S. Wu, Q. Liu and S. L. Shi, Amygdalin isolated from *Amygdalus mongolica* protects against hepatic fibrosis in rats, *Acta Pharm.* **71** (2021) 459–471; <https://doi.org/10.2478/acph-2021-0022>
13. H. M. Hao, X. Y. Jia, H. B. Zhou, W. F. Bai, H. Chang and S. L. Shi, Investigation of the anti-renal fibrosis effect of *Amygdalus mongolica* using metabolomics, *Acta Pharm. Sin.* **55** (2020) 1–18; <https://doi.org/10.16438/j.0513-4870.2020-0627>
14. Y. S. Zhao, P. S. Wu, H. W. Zhou, X. H. Cheng, S. L. Shi, Q. L. Li and H. B. Zhou, Studies on dose-effect relationship of *n*-butanol extracts of *Amygdalus mongolica* on reducing blood lipid and its chemical constituents, *Sci. Technol. Food Ind.* **38** (2017) 348–352; <https://doi.org/10.13386/j.issn1002-0306.2017.03.059>
15. W. F. Bai, Q. Liu, H. Chang, Q. L. Liu, C. Gao, Y. C. Bai, H. B. Zhou and S. L. Shi, Metabolomics reveals the renoprotective effect of *n*-butanol extract and amygdalin extract from *Amygdalus mongolica* in rats with renal fibrosis, *Artif. Cells Nanomed. Biotech.* **49** (2021) 556–564, <https://doi.org/10.1080/21691401.2021.1952212>
16. H. Chang, Q. Liu, W. F. Bai, Y. C. Bai, X. Y. Jia, C. Gao, Q. L. Liu, S. L. Shi and H. B. Zhou. Protective effects of *Amygdalus mongolica* on rats with renal fibrosis based on serum metabolomics, *J. Ethnopharmacol.* **257** (2020) 112858; <https://doi.org/10.1016/j.jep.2020.112858>
17. A. Burianni, M. L. Garcia-Bermejo, E. Bosisio, Q. Xu, H. Li, X. Dong, M. S. Simmonds, M. Carrara, N. Tejedor, J. Lucio-Cazana and P. J. Hylands, Omic techniques in systems biology approaches to traditional chinese medicine research: present and future, *J. Ethnopharmacol.* **140** (2012) 535–344; <https://doi.org/10.1016/j.jep.2012.01.055>
18. L. Shang, S. L. Yang, R. Yi and Y. L. Feng, Application of metabolomics and related technologies in research and development field of traditional chinese medicine, *China J. Chin. Materia Med.* **43** (2018) 4182–4191; <https://doi.org/10.19540/j.cnki.cjcm.20180709.005>
19. Y. Nan, X. Zhou, Q. Liu, A. Zhang and X. Wang, Serum metabolomics strategy for understanding pharmacological effects of *ShenQi* pill acting on kidney yang deficiency syndrome, *J. Chromatography B* **1026** (2016) 217–226; <https://doi.org/10.1016/j.jchromb.2015.12.004>
20. A. Nogueira, M. J. Pires and P. A. Oliveira, Pathophysiological mechanisms of renal fibrosis: a review of animal models and therapeutic strategies, *Vivo* **31** (2017) 1; <https://doi.org/10.21873/in-vivo.11019>
21. R. A. Gismondi, W. Oigman, R. Bedirian, C. R. Pozzobon, M. C. B. Ladeira and M. F. Neves, Comparison of benazepril and losartan on endothelial function and vascular stiffness in patients with type 2 diabetes mellitus and hypertension: a randomized controlled trial, *J. Renin Angiotensin Aldosterone Syst.* **16** (2015) 48; <https://doi.org/10.2174/1874192401610010212>

22. Z. H. Zhang, M. H. Li, D. Liu, H. Chen, D. Q. Chen, N. H. Tan, S. C. Ma and Y. Y. Zhao, Rhubarb protect against tubulointerstitial fibrosis by inhibiting TGF-beta/Smad pathway and improving abnormal metabolome in chronic kidney disease, *Front Pharmacol.* **9** (2018) 1029; <https://doi.org/10.3389/fphar.2018.01029>
23. M. Zhu, J. Du, A. D. Liu, L. Holmberg, S. Y. Chen, D. Bu, C. Tang and H. Jin, L-Cystathionine inhibits oxidized low density lipoprotein-induced thp-1-derived macrophage inflammatory cytokine monocyte chemoattractant protein-1 generation via the NF-kappaB pathway, *Sci. Rep.* **5** (2015) 10453–10462; <https://doi.org/10.1038/srep10453>
24. H. D. Wang, M. Yamaya, S. Okinaga, Y. X. Jia, M. Kamanaka, H. Takahashi, L. Y. Guo, T. Ohruji and H. Sasaki, Bilirubin ameliorates bleomycin-induced pulmonary fibrosis in rats, *Am. J. Respir. Crit. Care Med.* **165** (2002) 406–411; <https://doi.org/10.1164/ajrccm.165.3.2003149>
25. X. Wang, T. Wang, C. Zhang, F. Liu and C. M. Fu, Study on influence of magnolia officinalis before and after “sweating” on gastrointestinal motility disorder in rats by metabolomics, *Zhongguo Zhong Yao Za Zhi* **44** (2019) 1170–1178; <https://doi.org/10.19540/j.cnki.cjcm.20181225.001>
26. F. Rizvi, A. Defranco, R. Siddiqui, A. Holmuhamedov, L. Emelyanova, G. Ross, E. Holmuhamedov, P. Werner, A. J. Tajik and A. Jahangir, Simvastatin inhibits human atrial fibroblast proliferation through cell-cycle regulating cyclins by mevalonic acid-dependent pathway, *J. Am. College Cardiol.* **67** (2016) 670; [https://doi.org/10.1016/S0735-1097\(16\)30671-4](https://doi.org/10.1016/S0735-1097(16)30671-4)